FRICTIONAL BEHAVIOUR OF THE INTERFACE IN SiC MONOFILAMENT MODEL COMPOSITES WITH BOROSILICATE GLASS MATRIX

H. Cherouali, N. Louet, P. Reynaud and D. Rouby

Groupe d'Etudes de Métallurgie Physique et de Physique des Matériaux
GEMPPM UMR CNRS 5510, INSA de Lyon,

SUMMARY: A better knowledge of the cyclic fatigue effects in ceramic matrix composites needs a deeper understanding of the microscale mechanisms operating during friction between fibre and matrix. The present work deals with single filament model composites submitted to push-out tests at room temperature. Emphasis is made here on the effect of sliding velocity. The monofilament composites are made with a borosilicate glass matrix (Pyrex) and two types of silicon carbide filaments: SiC SCS-6 from Textron (coated with 3 μm pyrocarbon) and SiC Sigma from BP (nominally uncoated). The composites have been tested by a succession of push-out and push-back runs. The changes of frictional force are analysed as the drive velocity is suddenly changed: the SCS-6/Pyrex system exhibits the well known velocity weakening whereas an opposite behaviour is observed with the Sigma/Pyrex system. Qualitative and quantitative aspects of these results are discussed as regards to the mechanisms operating at the contact between the sliding surfaces.

KEYWORDS: glass matrix, silicon carbide monofilament, push-out test, interface behaviour, dry friction, stick-slip, sliding velocity, tribology.

INTRODUCTION

Ceramic matrix composites exhibit good resistance against damage extension, mainly because the fibres bridge the matrix cracks. The crack bridging efficiency is critically dependent upon the characteristics of the fibre/matrix interface. It is now well established that the cyclic fatigue behaviour of these composites is directly linked to the reduction of the stress transfer capability at the bridging, due to some wear phenomena in the sliding debonded zone [1, 2].

Therefore, a better knowledge of the cyclic fatigue life needs a deeper understanding of the frictional mechanisms operating during the cyclic friction between fibre and matrix. This is the main motivation of the present work which deals with single filament model composites submitted to push-out tests at room temperature under dry (unlubricated) friction condition.

After a brief description of the experimental push-out procedure and of the tested specimens, we will summarise the main features of the push-out behaviour as observed in these model systems. Actually, two filaments have been used. The difference between them is principally the presence or the absence of a pyrocarbon-coating layer and they will be described in more detail in the next section.

The aim of the present paper is to present some results obtained by imposing to the filament undergoing push-out a series of velocity jumps (of about one order of magnitude). The goal of

this study is to contribute to a better knowledge of the friction mechanisms operating at the scale of the contacts between the asperities of the sliding surfaces. This kind of information is necessary for a further study of the interfacial wear or abrasion phenomena, which control the cyclic fatigue lifetime in CMC's.

EXPERIMENTAL PROCEDURE

Push-out device

The tests are performed with an instrumented indentation device (see Fig. 1). The indenter is a WC/Co cylinder (6 mm diameter) equipped at its end with a conical tip (base diameter: 1 mm, angle: 30°). The tip of the cone is machined in order to get a flat pushing surface of about 50 to 80 μm diameter. The displacement is measured by means of a capacitive transducer placed very closely to the indenter axis. The force is measured each 0.1 μm. The special feature of this device is that the overall stiffness (including the frame, the load cell, the indenter tip and the specimen) can be easily changed. Coil springs of flexural beams of different sizes are used for this purpose, placed in series with the load cell (Fig. 1, right). The effective stiffness of the whole device, noted K, can be changed from 30 up to 1200 N/mm. The drive speed, given by a stepped micrometric motor table, is nominally 1 μm/second and can be changed by jumps.

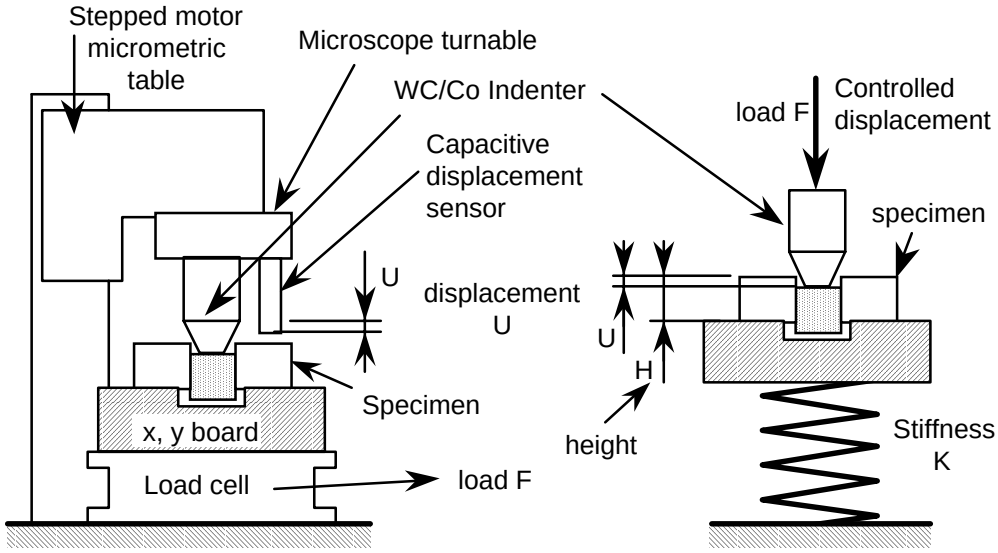

Fig. 1: Schematic representation of the push-out set-up

Specimens

The monofilament composites used in this study are made with a borosilicate glass matrix (Pyrex 732-01, from J. Bibby Science Products) and two kinds of Sic filaments: SiC SCS-6 from Textron Speciality Materials and SiC Sigma from British Petroleum. These filaments have been described in ref. 3. Shortly, the SCS-6 filament has a diameter of 140 μm and is coated with a pyrocarbon layer (3 μm thickness) containing SiC nanoscale SiC particles. The roughness of this filament is of 200 nm peak amplitude with an apparent wavelength of 10 μm. The Sigma filament (diameter: 100 μm) is uncoated and more rough (larger peak amplitude: 450 nm, lower apparent wavelength: 5 μm).

The composites are processed by hot pressing, the filament being placed between two Pyrex plates (pressure: 1 MPa, temperature, 810°C, duration: 30 min). After cooling, the composite plate is carefully cut perpendicularly to the filament axis, by means of a diamond wire saw, into small slabs with a thickness, noted H, of about 1 mm.

The testing procedure consists of submitting the specimen to a series of push-out/push-back cycles. The specimen is placed on the holder, centred relatively to a clearing grove of 300 μm width and depth and the filament is pushed out (first push-out run). The specimen is then turned, centred again and pushed back (first push-back). It is turned again in its original sense and pushed out again (second push-out), and so on.

TYPICAL PUSH-OUT BEHAVIOUR

During a push-out test, the applied load F is related to the interfacial shear stress τ (assumed here to be constant along the fibre) by:

$$F = 2 \pi R (H - U) \tau \quad (1)$$

With R: filament radius, H: specimen thickness, U: displacement of the fibre end. The measured displacement includes the fibre end displacement (several times 10 μm) and the crushing displacement of the indenter tip (about 1 μm under peak applied load). This error can be considered as negligible during friction under nearly constant F.

Assuming Coulombic friction law, the interfacial shear stress is related to an effective friction coefficient μ, by:

$$\tau = - \mu \sigma_{rad} \quad (2)$$

where σ_{rad} is the filament clamping stress which is due to a mismatch of the thermal misfit and a radial dilatancy resulting from the fact that sliding needs to overcome the height of the roughness asperities (see Fig. 2b). From the above expressions, a change in F can be due either to a change in friction coefficient or in clamping stress (or a change of both).

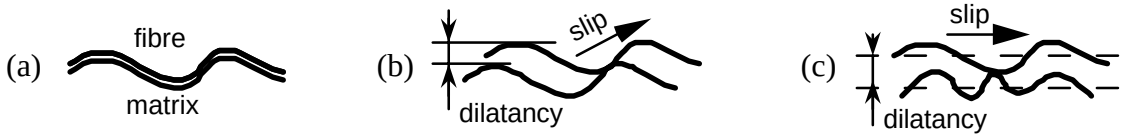

Fig. 2: Interaction between the asperities of the fibre and matrix surfaces. (a): coincidence; (b): short range sliding; (c): long range sliding.

As shown in Fig. 3, the push-out force as a function of fibre displacement exhibits a seating drop when the fibre reaches again its initial position. This phenomenon illustrates clearly the role of the roughness as two identical surfaces (mirrored by the hot pressing) begin to slide one over the other (Fig. 2b), or return in coincidence (Fig. 2 a). The seating drop has been analysed elsewhere [4].

The effect of interface degradation can also be seen in Fig. 3: for the SCS-6/Pyrex system, the overall friction curve decreases progressively as sliding proceeds. The load is always decreasing, so the reduction in interfacial shear stress τ, due to the wear, is more important than the cyclic change of the sliding area (the term $2 \pi R (H - U)$ in Eqn. 1). The interfacial shear stress decreases because of a wearing down of the roughness amplitude, leading to a decrease in the radial dilatancy and hence in the clamping stress (Eqn. 2). In addition, the wear debris can play a role of lubricant, leading to an eventual reduction in friction coefficient.

In the case of the Sigma/Pyrex system, it was observed that the friction force drops only at the start of the test because of the initiation and growth of some radial cracks in the matrix. Contrary to the SCS-6 filament, no significant wear has been noticed with the Sigma filament. This is probably due to the absence of a thick coating on that filament. The large roughness amplitude of the Sigma filament leads to well pronounced seating drop and post-seating peak (see top of Fig. 4). In addition, because of the same reasons, the push-out curve exhibits some

undulations appearing very reproducible from one run to another. This is an approximate picture of the effective wavelength of the roughness.

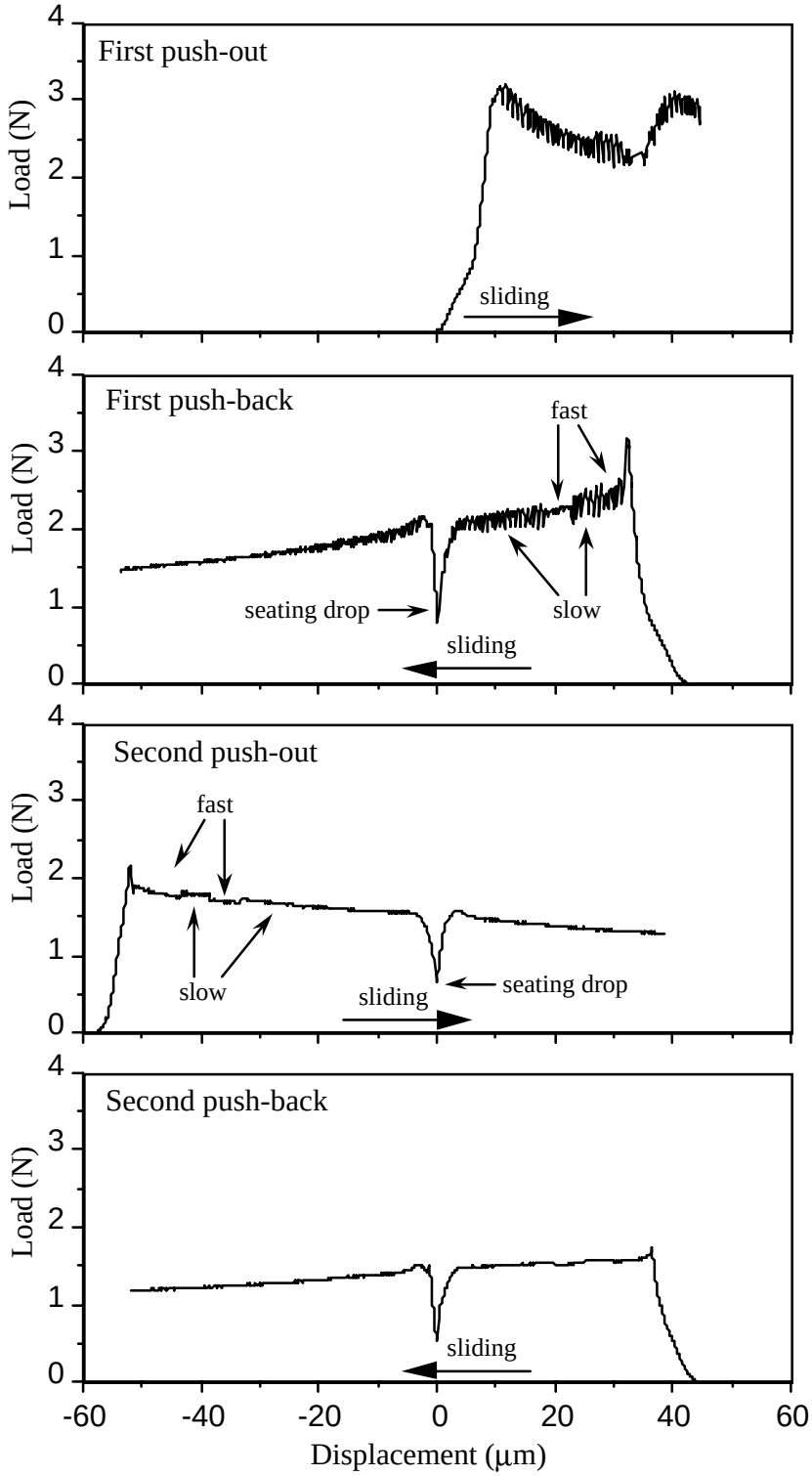

Fig.3: Typical succession of push-out/push-back runs (from top to bottom). SCS-6/Pyrex system (wet). H = 1000 μm, K = 1050 N/mm. Velocity: fast V = 1 μm/s; slow V = 0.2 μm/s (same displacement scale for all graphs)

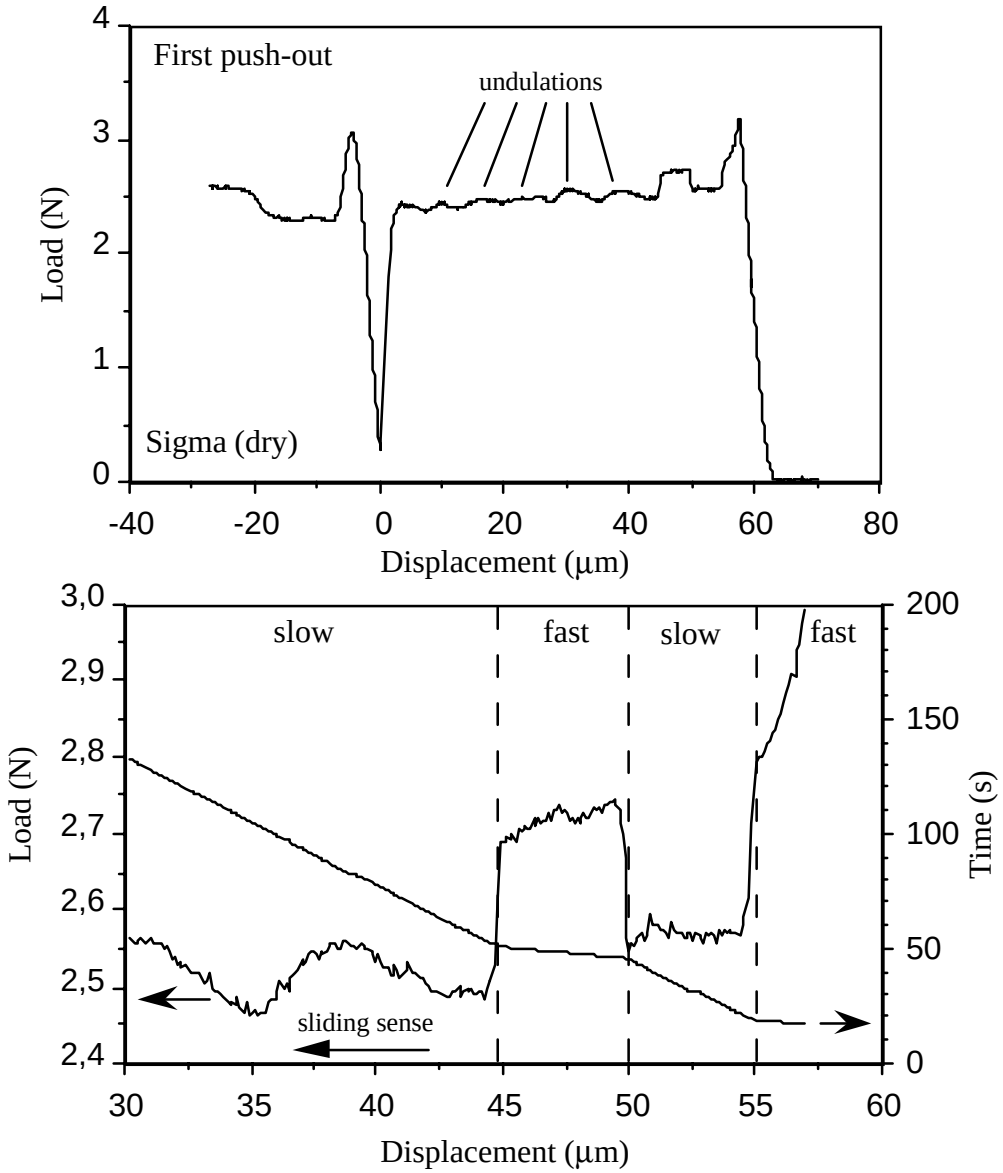

Fig. 4: Sigma SiC/Pyrex system (dry). Push-out force as a function of fibre displacement. H = 980 μm, K = 1050 N/mm. Velocity: fast V = 1 μm/s; slow V = 0.2 μm/s (the bottom figure is a magnification of the top one, giving detail of velocity steps)

The SCS-6 and Sigma filaments are also different as regards to stick-slip. Under standard dry friction conditions (the specimen being dried 2 or 4 hours at 150°C), the SCS-6 system exhibits a very regular stick-slip under low stiffness (K < 600 N/mm). With the actual stiffness (K = 1050 N/mm) the curve presents no serration (see Fig. 5). On the other hand, the Sigma filament exhibits erratic unstable slips only when K < 40 N/mm. The stick-slip observed in Fig. 3 will be discussed later.

Stable/unstable bifurcation arises from the mismatch between the resistance of the system to slide (characterised by the intrinsic law, i.e. the sliding force behaviour under infinite stiffness) and the drive stiffness (given by K). When a given frictional event leads to an increment of displacement, unstable slip occurs when the resulting drop in resistance becomes deeper than the corresponding drop in driving force. This condition can be fulfilled for geometrical reasons. For example, the entry in seating (Fig. 4) gives generally an unstable drop, the so-called seating drop. The above mentioned undulations can give rise to unstable slip when the stiffness K becomes smaller than the value of the slope at the inflexion point of the undulation [3].

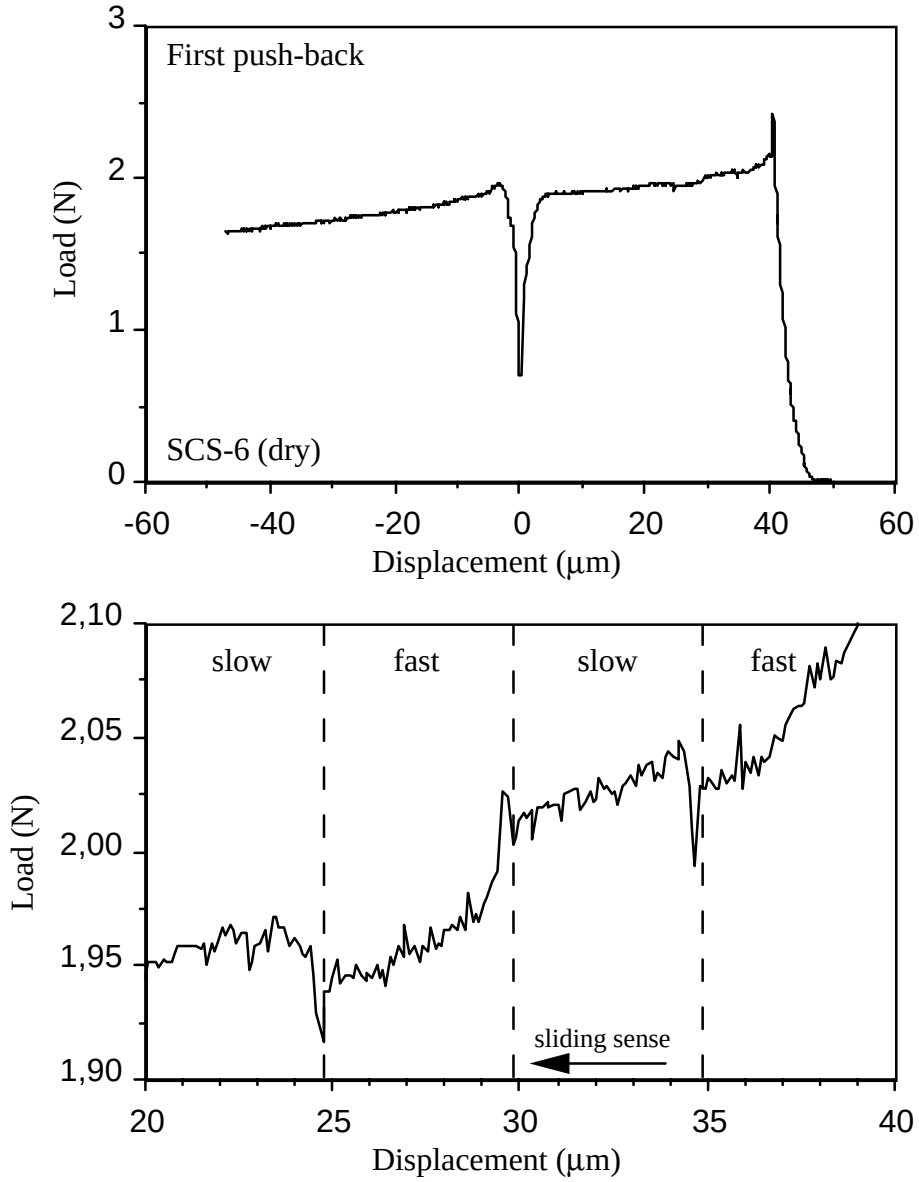

Fig. 5: SCS-6/Pyrex system (dry). Push-out force as a function of fibre displacement. H = 1010 μm, K = 1050 N/mm. Velocity: fast V = 1 μm/s; slow V = 0.2 μm/s (the bottom figure is a magnification of the top one, giving detail of velocity steps)

The above condition can also be fulfilled when the system exhibits velocity weakening. In that case, the stick-slip leads to quasi-periodic serration like those observed with the SCS-6 filament. It is well established that, in a lot of cases, the friction coefficient becomes lower as the sliding velocity increases. Actually, as the velocity increases, the contact time decreases and the current local contacts have not the time to develop higher strength for chemical or physical reasons [5]. An example of contact time influence can be described as follows. Under the normal pressure (the radial clamping stress) there is a crushing of the contacting asperities controlled by radial creep. So, the longer the contact time the larger is the real contact area and hence the contact strength [6].

Recently, Heslot et al. [7] proposed a model involving local creep phenomena for explaining the relation between velocity weakening, stiffness and unstable slip. The basic idea is the following: under the applied shear load at the end of the “stick phase”, shearing creep takes place at the level of the contacts leading to accelerating displacement and corresponding decreasing sliding resistance down to instability (the “slip phase”). According to that model, a

critical stiffness giving the bifurcation between stick-slip and steady sliding can be expressed as follows:

$$\text{Unstable if } K < K^*, \quad K^* = - \frac{2 \pi R (H - U) |\sigma_{rad}|}{U_0} \frac{d\mu}{d(\ln V)} \tag{3}$$

with $d\mu/d(\ln V)$: sensitivity of the friction coefficient to sliding velocity (negative) and U_0: average shearing displacement needed to break a contact.

The behaviour given by Fig. 3 has been obtained with the SCS-6 filament under wet condition (the specimen was placed a long time in water). In this case, stick-slip occurs even under high stiffness. This means that the current K (here 1050 N/mm) is a bit lower than K* and we can conclude that the velocity weakening effect ($d\mu/d(\ln V)$ term in Eqn. 3) is enhanced by wetting. Figure 3 shows also that the stick-slip progressively disappears as the sliding distance increases. This feature is an effect of wear which reduces K* through the reduction in clamping stress. The Heslot's model predicts also a decrease of the critical stiffness K*. This is qualitatively observed in Fig. 3 during the first push-back where fast sliding exhibits a less pronounced stick-slip. In the next section we will analyse in more detail the effect of velocity.

EFFECT OF SLIDING VELOCITY JUMPS

In order to have direct evidence of velocity effects on the sliding force, the push-out runs have been performed with drive velocity jumps at constant intervals of displacement. The SCS-6 and Sigma filaments exhibit very different responses to these jumps, as expected from the stick-slip behaviour.

In the case of the SCS-6/Pyrex system, the behaviour is very similar to that observed when rocks, ceramics [6] or Bristol paper [7] pieces slide together. As shown in Fig. 5 and 6, when the velocity is dropping off (by a factor 5 in the present case) the load exhibits first a sudden drop and then increases up to reaching a new value of stationary load which is higher than that corresponding to the previous velocity. The changes of the force are inverted when the velocity rises suddenly.

As discussed in the preceding section, the slowly sloping down of the friction force is due for a large part to wear, so the comparison of the fast and slow levels must be made as regards to an oblique baseline. For the velocities used here we find:

$$\frac{dF}{d(\ln V)} = - 0{,}015 \pm 0{,}003 \text{ N} \tag{4}$$

The influence of wear on this ratio was not measured systematically. In conclusion, the SCS-6/Pyrex system exhibits a typical velocity weakening behaviour. As mentioned before, this effect can be explained by the duration of the solid-solid contacts (the "age" of the current contact population) linked with the indentation creep dynamics in which the area of the contacts increases with time. For a given intrinsic strength of the contact, the friction resistance is directly linked to the contact area that is rising with contact time (an "older" contact is stronger). Because the contact time is inversely proportional to the velocity, the friction coefficient exhibits a velocity weakening.

The abrupt drop of load just at the velocity jump indicates the presence of another mechanism: the mean strength of the contacts, which population is of the same "age", increases with loading rate. This observation, very general in materials science, suggests that the intrinsic contact strength could be controlled either by sub-critical crack growth (brittle behaviour) or by time dependent micro-mechanical yield (ductile behaviour).

The load change (more soft in appearance) occurring just after the drop corresponds to the relative sliding displacement U* (and time) needed for changing the "age" of the contact population according to the new sliding velocity. Despite the scattering of the recorded dots we can estimate U* to about 0.5 to 1 μm (Fig. 5 and 6). It is interesting to compare this value

with U_0, the average shear displacement needed for breaking a contact by shear, introduced in the Heslot's model. By taking K* = 600 N/mm [3] and using the result given by expression (4), Eqn. 3 leads to the following value: U_0 = 26 nm, which is much lower than U*. In theory, U* and U_0 have the same meaning (changing the contact "age" needs to change the contacts, so the "old" contacts have to be broken) and the present discrepancy seems to indicate that an additional mechanism is operating. Notice that the Heslot's model do not take into account the existence of wear phenomena. More work should be done in this field, especially about the role of wear mechanisms on the threshold of unstable slip.

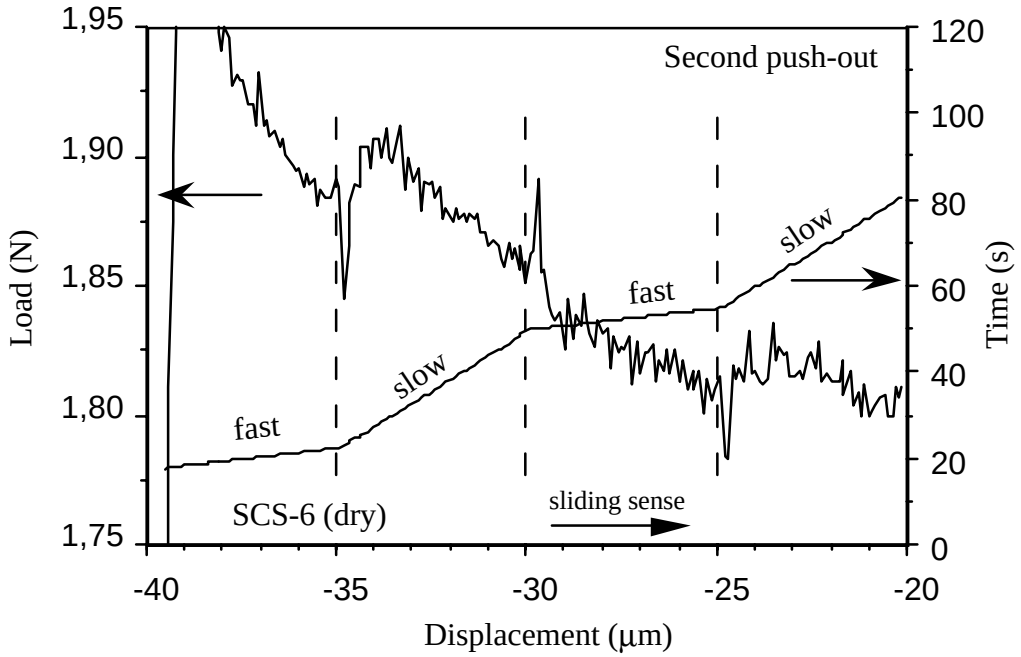

Fig. 6: SCS-6/Pyrex system (dry).
Detail of the velocity jump effects observed during the second push-out.
H = 990 μm, K = 1050 N/mm. Velocity: fast V = 1 μm/s; slow V = 0.2 μm/s

In the case of the Sigma/Pyrex system (Fig. 4), a positive rate sensitivity is observed during steady state friction. This explains the absence of dynamic stick-slip, even at very low stiffness. In this case the friction is directly concerned with the rate dependence of the contact strength controlled either by shearing of asperities for a ductile contact, or by asperity breaking for a brittle contact. An interesting discussion about these mechanisms is made by Estrin and Bréchet [8]. With the Sigma filament, no ageing process (by radial crushing or some other mechanism) of the contact is working. The cause of that is probably the absence of pyrocarbon interphase layer at the fibre surface. Notice also that this system presents no significant wear by abrasion of the asperities.

According to the analysis of Erstrin and Bréchet [8] for both ductile and brittle material behaviour, the overall friction behaviour in the steady state sliding can be described by means of a N-shaped curve.

Between V_1 and V_2 velocities, the frictional system is in the ageing regime: the contact "age" controls the strength of the contacts. This negative rate sensitivity regime holds for the SiC SCS-6/Pyrex composites for velocities around 1 mm/s. The ageing involves radial creep but the effect of moisture suggests that some chemical ageing (by time dependent creation of chemical links) is also working.

For $V > V_2$, the contact time being very short, the ageing have no time to take place. The strength of the contacts is therefore only controlled by the stressing rate in shear. Here, the rate sensitivity is positive and this velocity regime holds for the SiC Sigma/Pyrex composites,

where V_2 is lower than say 0.1 mm/s. For $V < V_1$, the contacts are fully aged and the strength is also controlled by the stressing rate (positive rate sensitivity). Presently, the arguments for placing the Sigma system in the high velocity regime are very weak and more work must be done, principally by exploring larger velocity domains and by studying the effect of chemical environment.

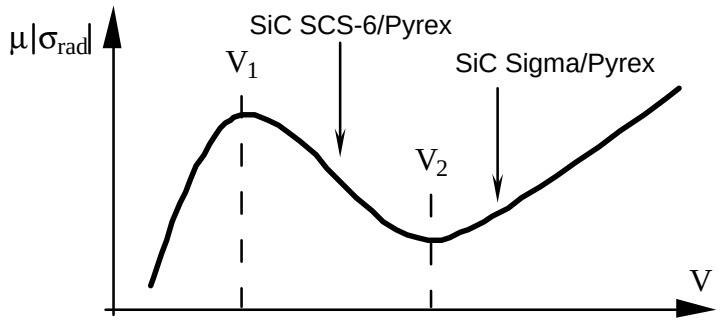

Fig. 7: Dependence of the friction coefficient or interfacial shear stress as a function of sliding velocity. SiC SCS-6/Pyrex: ageing regime; SiC Sigma/Pyrex: shearing regime

CONCLUSION

The above discussion shows clearly that the interface behaviour cannot be described with a Coulombic friction law between two perfect smooth surfaces. Because of the roughness a lot of additional features have to be considered: radial dilatancy and asperity crushing, sliding velocity and time dependent phenomena at the contacts, wear phenomena linked with the amount of relative displacement and of radial pressure.

Up to now the interface has been tailored in order to promote matrix crack deviation and resistance against oxidisation at high temperature under air. The key question for the next step is to improve the interface resistance against wear under cyclic loading. This problem of cyclic fatigue life becomes more and more important as the lifetime in oxidising atmosphere becomes longer, say 20.000 hours.

From a theoretical point of view, the features associated with the wear phenomena should be included in the models describing the dynamics of the dry friction behaviour. This must be the task concerning the interfaces in CMC's in the near future.

REFERENCES

1. Shuler, S.F., Holmes J.W. and Wu, X., "Influence of loading frequency on the Room-Temperature Fatigue of a Carbon-Fiber / SiC-Matrix Composite", *Journal of the American Ceramic Society*, Vol. 76, No. 9, 1993, pp. 2327-

2. Rouby, D. and Reynaud, P., "Fatigue behaviour related to interface modifications during load cycling in ceramic matrix composites", *Composite Science and Technology*, Vol. 48, 1993, pp. 109-118.

3. Cherouali, H., *Rôle des interfaces et de la rugosité dans le comportement interfacial de composites monofilamentaires à matrice fragile*. Thèse de Doctorat, INSA de Lyon (98ISAL0010), 1998.

4. Cherouali, H., Reynaud, P. and Rouby, D., "Interface roughness and sliding in ceramic matrix composites", *Damage and Failure of Interfaces*, A.A. Balkema, Rotterdam, H.P. Rossmanith, Ed., 1997, pp. 411-418.

5. Persson, B.N.J. and Tossati, E., *Editors, Physics of Sliding Friction*, NATO ASI Series E. 311., Kluwer Academic Press Pub., Dortrecht, 1996.

6. Dieterich, J.H. and Kilgore, B.D., “Direct Observation of Frictional Contacts: New Insights for State-Dependent Properties”, *Pure and Applied Geophysics*, Vol. 143, 1994, pp. 283-302.

7. Heslot, F., Baumberger, T., Perrin, B., Caroli, B. and Caroli, C., “Creep, stick-slip and dry-friction dynamics: Experiments and a heuristic model”, Physical Review E, Vol. 49, No. 6, 1994, pp. 4973-4988.

8. Estrin, Y. and Brechet, Y., “On a Model of Frictional Sliding”, *Pure and Applied Geophysics*, Vol. 147, 1996, pp. 283-302.